Optical investigation on the interaction between a fuel-spray and an oil wetted wall with the focus on secondary droplets

Malki Maliha[1] [ID], **Bastian Stumpf[2], Felix Beyer[1], Marius Kühnert[1],
Heiko Kubach[1]** [ID]**, Ilia Roisman[2], Jeanette Hussong[2]
and Thomas Koch[1]**

Abstract

Since the technology of direct injected engines has become more and more prevalent, combustion anomalies such as pre-ignition events have been occurring with increasing frequency. The interaction between the fuel-spray and the oil wetted cylinder liner is considered to be a partial cause for these phenomena. The incoming fuel jet can lead to a detachment of secondary droplets, which may affect pre-ignition events due to their changed flammability properties. To characterize these secondary droplets, spatially and temporally highly resolved optical investigations on the fuel-oil-film-interaction are carried out in this work. Using laser induced fluorescence and two high-speed cameras both fluids are optically separated. Thereby the secondary droplets can be detected and characterized in size, velocity vector, and composition.

Keywords

Pre-ignition, fuel-wall-interaction, LIF, secondary droplets, fuel jet

Introduction

The CO_2 reduction is the main development driver since many years. Downsizing has become a widespread optimization method, as it can help to improve efficiency and thus reduce fuel consumption and CO2 emissions. It led to the use of low-displacement gasoline engines with a multi-hole direct injection. Because in a direct-injected engine, the fuel interacts strongly with the oil-wetted cylinder wall, the influence of fuel-wall-interaction on the combustion behaviour is steadily increasing and thus becoming the focus of scientific investigations. The downsizing of gasoline engines increases the efficiency due to higher specific load. However, it affects the behaviour of combustion anomalies such as knocking and, due to the fuel-wall-interaction also pre-ignition events.[1] Especially the causes of pre-ignition phenomena are not fully understood yet and are increasingly observed in connection with the internal mixture formation. In addition to flaking pieces of combustion chamber deposits,[2,3] oil droplets detached by the fuel are suspected to influence

these phenomena.[4,5] Therefore, the formation mechanism and the characterization of these secondary droplets need to be investigated in detail. The interaction of droplets on surfaces and fluid films are well described in the literature.[6–21] The droplet impact and rebound as well as the surface wetting of dry walls is described from Richter.[6] The interaction between a droplet and a fluid film is highly influenced by the droplet size to film thickness ratio. Furthermore, the physical properties of both fluids affect the interaction phenomena. For this purpose, a droplet-liquid-interaction was studied with the same fluids[7,8] and with

[1]Institute of Internal Combustion Engines (IFKM), Karlsruhe Institute of Technology (KIT), Karlsruhe, Germany
[2]Institute of Thermo-Fluids & Interfaces (TFI), Technical University of Darmstadt (TUD), Darmstadt, Germany

Corresponding author:
Malki Maliha, Institute of Internal Combustion Engines (IFKM), Karlsruhe Institute of Technology, Rintheimer Querallee 2, Gebäude 70.03, Karlsruhe, Baden-Württemberg 76131, Germany.
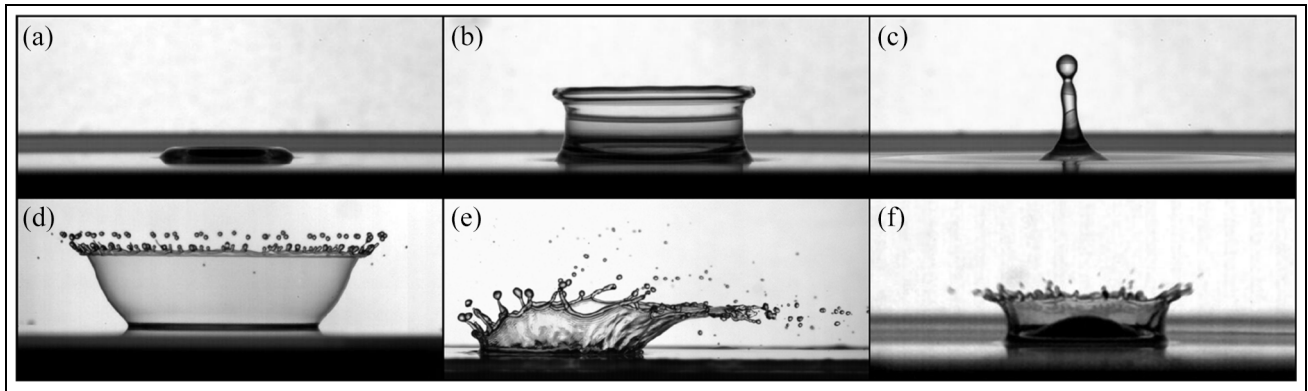Email: malki.maliha@kit.edu

Figure 1. Summary of drop impact outcomes: (a) Deposition (Silicone oil, Re=150, We=76.3, H=0.33, t=4.35 ms); (b) Corona Formation (Silicone oil, Re=450, We=686.4, H=0.33, t=7,5 ms); (c) Partial rebound (Silicone oil, Re=450, We=686.4, H=0.33, t=30.8 ms); (d) Corona Splash (Silicone oil, Re=600, We=950, H=0.045, t=1.8 ms); (e) Inclined impact with corona splash and prompt splash (Water-urea Solution, Re=7724, We=452.3, H=0.071, t= 3.2 ms); (f) Corona formation with prompt splash and rim instability (Water, Re=6900, We=395.9, H=0.087, t=0.6 ms). The time t describes the time from the moment of impact. Drop and film are of the same liquid.

different non-miscible fluids.[9,10] Thereby the conditions for the formation of droplet detachment and their properties could be determined. On the other hand, a spray array behaves very differently to the single droplet process due to neighboring droplets influencing each other. The interaction of a droplet array on liquid film is also investigated and described in the literature,[8,11,12] however not with engine-relevant boundary conditions. The fuel spray, used in this work, contains droplets varying greatly in size, velocity, and spatial distribution and is generated by a modified series production GDI injector. Furthermore, the impact angle with the liquid is set to 45°. The used fluids are RON95 for the fuel-spray and an engine oil for the liquid film lying on the wall. In this work, the development of the experimental setup to observe such an interaction is described in detail. In addition to the LIF utilized, the focus is on the optical setup consisting of high-speed camera, objective and optical filter. With this setup it is possible to separate both fluids optically and perform a macroscopic analysis on the interaction phenomena. In the literature engine-relevant and multicomponent fluids RON95 and engine oil are poorly described, especially with respect to the interaction processes. The literature mainly uses single-component reference fluids. Furthermore, the use of the fluorescent tracers selected here is novel and not described in literature before.

State of knowledge

Pre-ignition phenomena

Internal combustion engines with a spark ignition principle are subject to combustion anomalies. The most common and therefore well studied are knocking effects. Uncontrolled self-ignition occurs in the unburned mixture due to high pressure and temperature This can lead to high peak pressures and pressure

gradients and thus to mechanical damage to the engine. These phenomena can be prevented by load reduction or delayed ignition. In this case it is possible to reduce or even prevent these harmful effects by active intervention. Pre-ignition phenomena differ in principle and prevention strategy clearly from knocking. These effects occur stochastically as single or multiple events. They are characterized by an early start of ignition, even before ignition time, and thus lead to fast combustion and extremely pressures. These pressures can exceed the permissible peak pressure by more than 100 bar and therefore cause an engine damage even by rare occurrence. They cannot be prevented by ignition adjustment. It seems they are caused by an external ignition source such as small flaking pieces of combustion chamber deposits (CCD). The resulting pressure gradients can detach further pieces of CCD and lead to more pre-ignition events. These events then occur until the reservoir of CCD is completely depleted.[2–4] However, a detached oil droplet, as a result of a spray-wall interaction, cannot be excluded as an ignition source for the initial or a single pre-ignition event.[4,5]

Droplet-fluid interaction

The impact of a droplet on a dry or wetted surface is the subject of widespread investigations. This interaction is highly influenced by many conditions such as number of interacting droplets, size ratios, impact angle, fluid properties, etc.[13] This work focused on the formation or detachment of secondary droplets as a result of a droplet impact.

The impact of a droplet can lead to detachment of liquid droplets and thus to the formation of a secondary spray. There are different mechanisms that can result in droplet detachment.[14] The phenomenon best described in the literature is corona splashing on thin liquid films, as shown in Figure 1(d)–(f). In the figure shadowgraph images of drop impact outcomes in
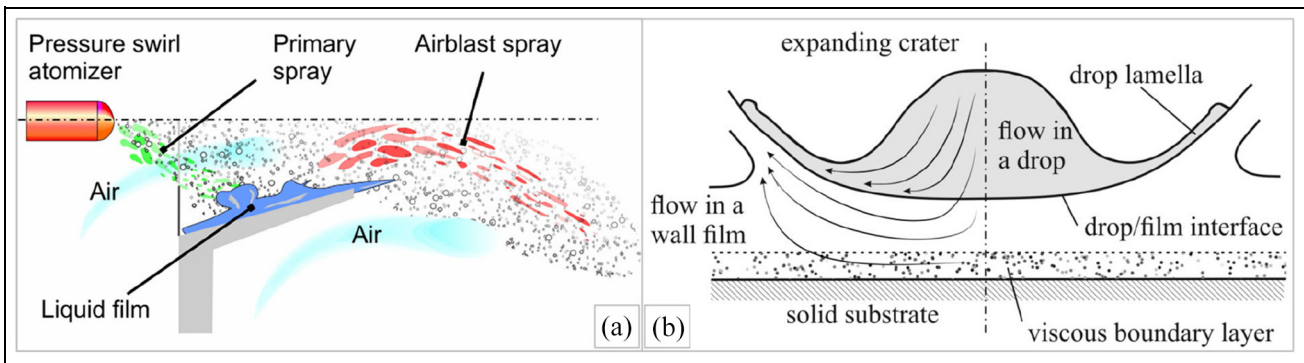
Figure 2. (a) Model of an air blast atomization process and (b) Distribution during drop impact on liquid film with different fluids.

different regimes are presented. The images are obtained with an high-speed camera system utilizing a Photron SA-X2 CMOS camera with framerates of up to 50000 fps. The drop is generated by a drop on demand system and then accelerated by gravity until it impacts onto a liquid film. In Fig 1 a)-d) and Fig 1 f) the drop impacts onto a horizontal, liquid film. In Fig 1 e) the drop impacts onto an inclined liquid film with an inclination angle of 40°.

At the point of impact, the fluid is displaced, resulting in a thinner layer compared to the initial film. The radially initiated flow leads to the formation of a crown, which is strongly dependent on the impact conditions. A characteristic rim at the tip of the crown, which can be unstable under certain conditions, can in turn lead to the formation of small cusps. These develop into fingers before secondary drops can detach.[6–9] Boundary conditions leading to the occurrence of corona-splashing are mainly size and velocity vector of the impinging droplet and thickness of the liquid film, but also physical properties such as kinematic viscosity or surface tension. According to Kubach et al.,[4] the probability for the occurrence of corona splashing increases with droplet size and velocity. However, a thicker liquid film reduces the probability of occurrence for secondary droplets due to corona splashing.[4] The angle of impact of the incident droplet significantly affects the impact and crown shape.[13,15,16] An inclined drop impact can lead to an asymmetrical formation of the crown, which influences its stability and thus also the secondary drop formation, what is shown in Figure 1(e)). This can lead to a change in the critical splashing thresholds. According to Liang and Mudawar,[13] Liang et al.,[17] Sikalo et al.,[18] the threshold for inclined drop impact can be defined by a multiplication of the commonly used Weber number, with the factor $\sin^2\Phi$ which takes the angle of impact into account. Since the factor $\sin^2\Phi$ is smaller than 1, the probability of occurrence of corona splashing increases with increasing impact angles.

In addition to the impact of droplets on a thin liquid film, the interaction on thick, deep liquid films is also the subject of research and relevant for this work. Here, a relative film thickness of H > 1 (film/droplet) and above is referred to as a deep film.[6,19] The impact differs from the thin film in that it is not limited by the rigid wall in the impact direction. This influences the formation of the lamellae and the secondary droplets. According to Richter,[6] two different types of secondary droplets can form: By detachment at the crown tip and in the impact center by detachment of the resulting jet. These droplets differ in size and direction of movement.

Another phenomenon that leads to the detachment of secondary droplets is prompt splashing, what can be seen in Figure 1(f)). In this process, droplets are detached from the crown well before reaching their maximum height. As a result, the secondary droplets formed this way are much smaller than those formed by the corona splashing. Often, the spontaneous splashing is followed by the previously described droplet detachment at maximum crown height. These effects occur more frequently with low viscosity liquids.[9,13]

The impact of droplets on liquid film with different fluids is more complex and significantly affects the formation of the characteristic lamella and secondary droplets.[9] considers the different fluids mainly by the ratio of viscosities (film to droplets). It is described that lower viscosity ratios lead to a reduction of the maximum crown height. Also, an increased stability of the finger-like jets at low viscosity ratios and thus a lower tendency to splash can be observed. However, the phenomenon of spontaneous splashing can be observed more at low viscosity ratios. Furthermore, the miscibility of the different fluids influences the formation and composition of the secondary droplets. According to Kittel et al.,[10] geometric parameters, such as the relative film thickness, also influence the interaction conditions. As can be seen in Figure 2(b)), the crown can contain parts of both the incoming droplet and the initial film.

The fuel spray of a direct injected gasoline engine show a high droplet number density and high velocities with a very small droplet size. For this reason, the influence of adjacent droplets on the interaction must be considered. These phenomena are also well described in the literature by generic consideration. The simultaneous impact of multiple droplets is described by Roisman and
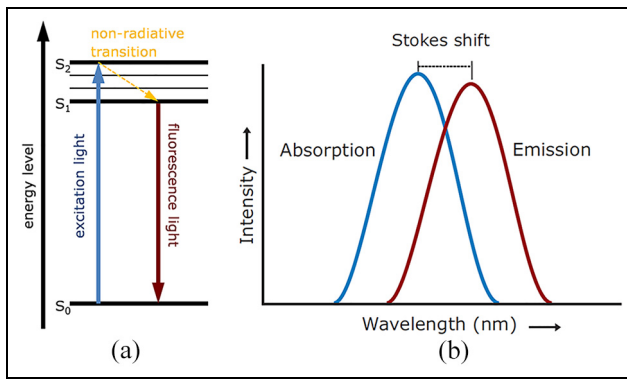
Figure 3. (a) Jablonski diagram (b) a principle stokes shift[22] to lower-energy light emission.

Tropea,[8] Sivakumar and Tropea,[11] Gianpietro et al.,[12] Liang and Mudawar[13] and it is observed that adjacent crowns can collide depending on the distance of the interactions, leading to the formation of secondary droplets. Furthermore, the film thickness between impact events can change depending on the interaction distance and reach a maximum at a distance of 2d. However, the time-shifted superposition of an interaction can also affect the impact phenomena. According to Richter,[6] an increased frequency of successive drops leads to the formation of smaller secondary drops. Furthermore, an increase of the impact velocity also leads to a reduction of the secondary droplet size.

Another detachment event described in the literature is detachment as a result of strong air currents or high liquid velocities, the so-called air-blast atomization.[20,21] Roisman et al investigated and modeled a spray impact on a liquid film under strong air flow. They were able to describe the detachment of droplets from the liquid film due to the air flow using the dimensionless Weber number of the air flow We_G. As can be seen in Figure 2(a),[20] the air-blast droplets are characterized by a relatively large droplet diameter. They can become as large as the thickness of the liquid film.

Laser-induced fluorescence (LIF)

Laser-induced fluorescence is a powerful, widely used tool for optical investigation of fluid dynamic, multiphase phenomena.[22–24] The physical basis of this principle is an energetic stimulation of certain molecules by a light source. In this process, electrons of the molecule to be stimulated are raised to an energetically higher level, from which they can return to their initial state by emitting a photon. Figure 3(a) shows this principle of LIF by means of the Jablonski diagram. Through various phenomena, the energy level of the excited electron can be partially reduced before a spontaneous emission of a photon occurs. This leads to the emission light being energetically poorer than the excitation light and thus a red shift can be observed. This shift, called stokes shift (see Figure 3(b)), should be large enough to allow a separation of the emissions spectra from the excitation spectrum. However, only specific molecules can be excited with specific wavelength, the absorption spectra. These molecules, which are added to the fluid to be investigated, are called tracer or laser dyes and must be carefully selected. Therefore, the tracer should be non-invasive and have a suitable solubility in the corresponding fluid, but at the same time be chemically stable in the emulsion so that the optical properties are not affected by the admixture. On the other side the concentration of the laser dye influences the emitted signal, even if the correlation is not linear.[24] Several quenching effects, which finally lead to a transformation of the absorbed energy into heat by intermolecular processes, might decay the emission light and thus reduce the fluorescence quantum yield.[25] Many boundary conditions such as tracer concentration, fluid temperature and ambient pressure can affect the fluorescence quantum yield and must be carried out carefully.

Experimental setup and analytical methods

Oil-film generation

The oil film inside an internal combustion engine is well investigated and described in the literature.[26] The film thickness can vary significantly at different operating points and even within one engine cycle. The level of thickness ranges mostly from 10 to 30 μm. To ensure the reliability and repeatability of the investigations an oil film generator was developed, which is able to generate continuously variable oil film thicknesses in the relevant range. A spin coater, driven by an electric motor, can rotate a sample plate, which is covered with oil. The spin coater is shown in Figure 4(a)). The centrifugal force, which is induced by the rotational movement, distributes the oil on the plate and removes the excess oil. This effect occurs until the adhesion and the centrifugal force balance each other or the rotation stops. The applied forces are also shown in Figure 4(a)). The oil film thickness is therefore a result of rotation speed and duration of the final speed. The start or stop ramp did not affect the oil film significantly. The parameter settings were determined and are shown in Figure 4(b)). It can be seen, that oil film thickness's between 10 and 60 μm can be generated continuously. Furthermore, the repeatability of the generation was investigated and a standard deviation of max. ±0.9 μm could be found out. A variability of the film thickness over the entire plate could not be observed. The film thickness is measured by means of laser absorption spectroscopy and is further described in van der Kley et al.[27]
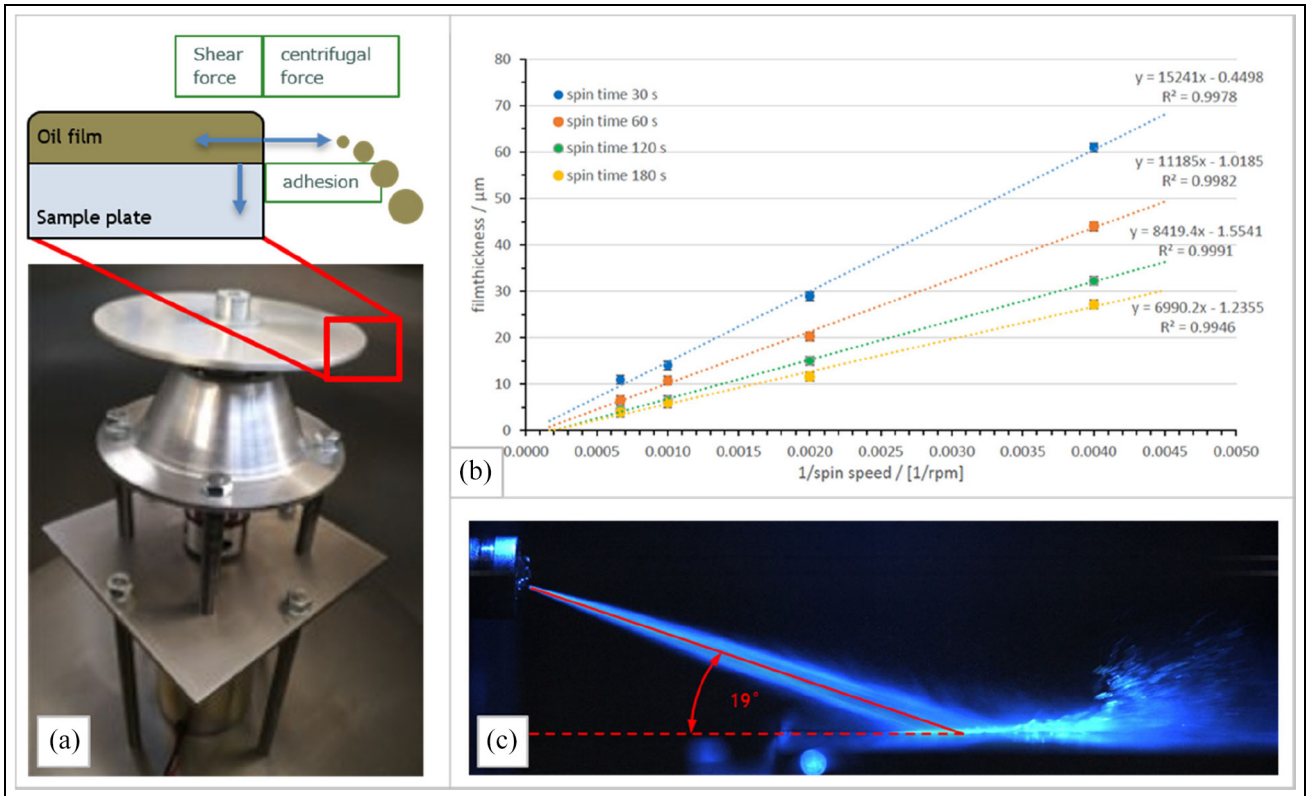
Figure 4. (a) spin coater and balance of forces which are responsible for the oil film generation (b) measurement of oil film thickness depending on the operating parameters of the spin coater with by means of laser absorption spectroscopy (c) generation of a single fuel jet with a BOSCH HDEV5.2-injector.
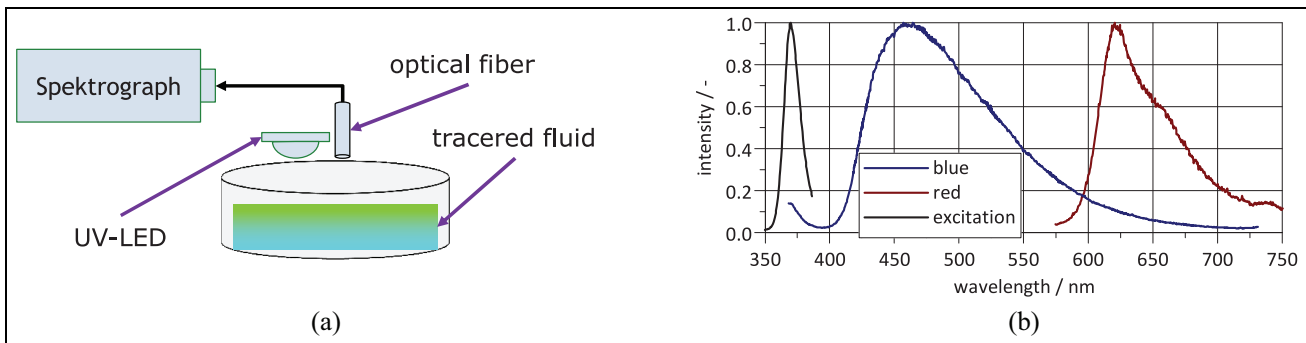

Figure 5. (a) a principle setup of spectroscopic investigation of LIF-tracers (b) spectra of the used light source and fluid tracer.

Fuel-jet generation: Injector, sealing off holes, alignment of injector

The fuel jet is generated by means of a Bosch HDEV5.2 GDI injector at a fuel pressure of 50 bar. This is a six-hole, solenoid injector and is made for a one litre inline three-cylinder engine with gasoline direct injection. Five holes were closed using a suitable gluing process to increase the optical access on the interaction of fuel jet and oil film. The orientation of the resulted single fuel jet is optically investigated to ensure a precise alignment. Figure 4c) shows the inclination of the jet with respect to the injector. Furthermore, the spray characteristics are investigated with a PDA System. However, the closing process of injection nozzles can affect the

characteristic of the fuel jet, which are described in detail in Maliha et al.[28]

Light source and tracer setup

A tracer had to be selected for each of the two fluids, oil and fuel. While the absorption spectra should be as similar as possible, the emissions spectra must be clearly spectrally shifted from each other. Therefore, two organic luminescent pigments, which are excited in the Ultra-Violette range, could be found and analysed. For their investigation, a specific experimental setup, shown in principle in Figure 5(a)), is needed. A fiber optic transmits the emitted light to a spectrograph and allows
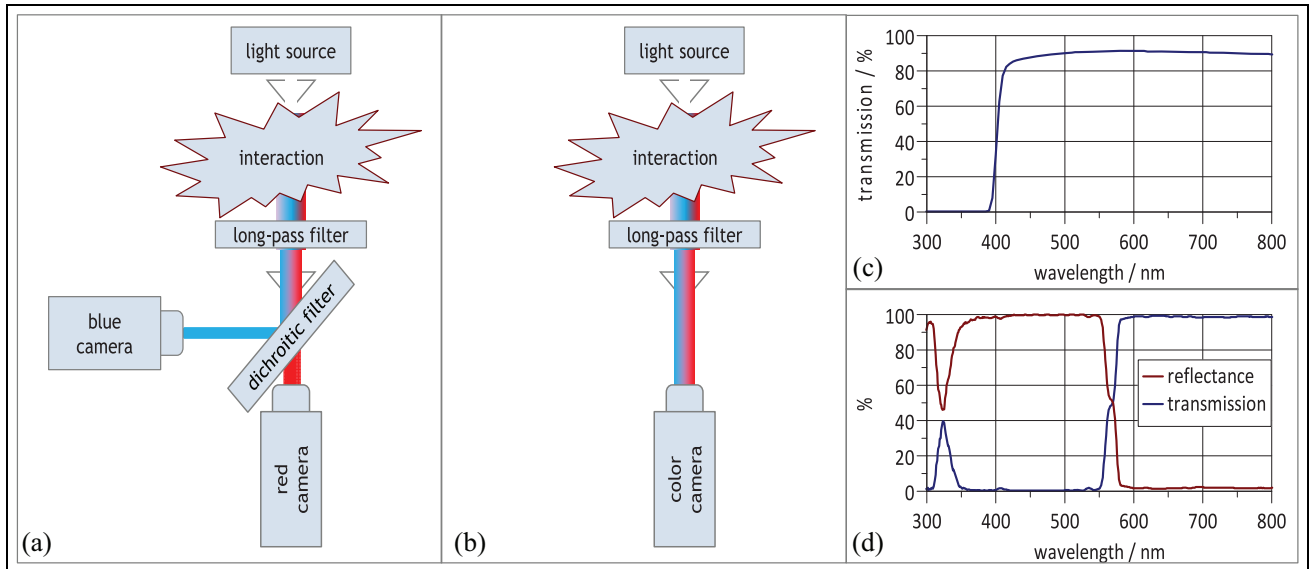
Figure 6. (a) Experimental setup for black-and-white imaging, (b) experimental setup for color imaging, (c) spectral properties of long-pass filter, and (d) spectral properties of second dichroic filter.

the spectrum to be recorded. The alignment of fiber optic and light source must be chosen carefully to prevent a direct incidence of excitation light into the spectrograph.[24] The spectra of the excitation and both tracers is shown in Figure 5(b)). The tracer used for the fuel emits blue light, while the tracer used for the oil emits red fluorescence light. Because the fluorescence intensity does not depend linearly on the dissolved tracer concentration in the fluid, the optimum admixture had to be investigated. 350 mg/L tracer was added to the fuel and 35 mg/L to the oil. A 10W ultra-violet light emitting diode (LED) was used as the excitation source, which has a peak wavelength of approximately 365 nm and a beam angle of 60°.

Alignment and optical filter setup

The layout of the several components was carefully adapted and developed. Two operation modes are chosen, one for the polychrome (Figure 6b) and one for the monochrome images (Figure 6a). The polychrome images are mainly used for a better visualization of the interaction processes. Furthermore, a higher temporal resolution is possible. The monochrome images provide more detailed information about the composition of the observed fluids. Moreover, a higher spatial resolution is possible. In addition, a naming convention is introduced that has the light source as the start and the cameras as the end point, see arrows in Figure 6a and 6b. For these setups, different optical filters are necessary to allow high quality imaging. After the interaction area, the excitation light is blocked by a long-pass filter (see Figure 6c) to observe only the fluorescent fluids. For the polychrome images, the lens and the camera are arranged after this long pass filter. The black-and-white recording requires another dichroic filter (Figure 6d) in front of the

cameras. It separates the fluorescent light by reflecting the blue light of the oil tracer to the first camera and transmitting the red light to the second camera.

Characterization of the spray interaction onto an oil film

As already described in Chapter 2.2, geometric and physical boundary conditions influence the interaction of a fuel spray with an oil film on a solid wall. The relevant boundary conditions for describing the interaction will be explained here. The oil film used has been generated with a thickness h of about 80 μm by setting the operating parameters of the spin coater according to Figure 4(b). This oil film thickness was chosen because it allowed high quality and assessable images with the current experimental setup. Future development should allow the oil film thickness to be reduced to engine-like 20 μm without compromising image quality. The single fuel jet from an HDEV5.2 injector used for this study is measured by means of a PDA and is described in detail in.[28] The spray consists of many droplets varying greatly in diameter and velocity. The fuel is injected in a calm atmosphere with atmospheric pressure and temperature. From these distributions, dimensionless indices can be calculated to characterize the interaction, as is common in the literature. Figure 7 shows the distribution of droplet sizes and the resulting relative film thickness H. This is determined by the ratio of oil film thickness to droplet diameter (h/d). It can be seen that the relative film thickness varies greatly and can take values between > 500 to about 1.3. In the literature, a significant change in the interaction processes is described from a relative thickness of approx. one. For a fictive oil film thickness of 20μm, values between approx. 200 and 0.3 would result for the relative film
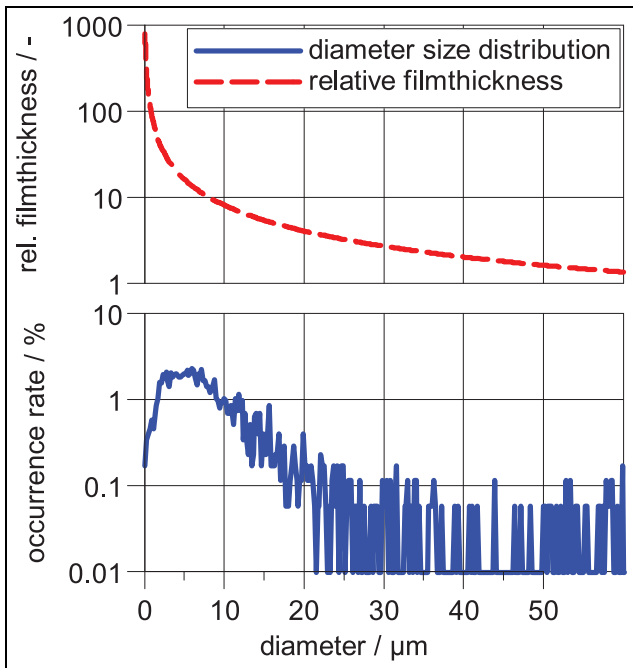
Figure 7. Occurrence rate of droplet size and the resulting relative film-thickness.

Table 1. Physical properties for calculation of dimensionless factor.

Fluid name	RON95
Density/kg/L	747
Surface tension/mN/m	20
Dynamic viscosity/mm^2/s	0.85
Impact angle/°	45
Earth acceleration m/s^2	9.81

thickness, which is why the interaction on thin as well as on thick liquid films could occur and have to be considered. Finally, the arithmetic means of the droplet size $d_{AMD} = 9.14\,\mu m$ and the relative film thickness $H_{AMD} = 18.63$ were calculated. Thus, for the processes considered in this work, the interaction of a spray on a thick, deep liquid film can be assumed.

Considering the droplet velocity distribution and the physical properties from Table 1, the dimensionless numbers Weber $We = \rho u^2 d/\sigma$, Froude $Fr = v/(gd)^{1/2}$, and Reynold $Re = du/v$ can be calculated for every droplet in the fuel spray. In the literature, the dimensionless factor $K = Re^{1/2} We$ is additionally used to determine the splashing thresholds, although mostly for the impact on thin films. Moreover, the influence of the impact angle of 45° according to[13,17,18] can be considered by calculating the modified Weber number $We' = We \sin^2\Phi$. Figure 8 shows the distribution of We', Fr, and the K-factor for the used fuel spray. It can be seen that the calculated dimensionless numbers can cover a wide range of values. As high Weber and Reynold numbers can be seen, splashing effects should be occur with high probability.

Table 2. Camera properties of several setups.

Camera	Phantom V1612	HSS6
Chip size	35.8 × 22.4 mm (1280 × 800)	20 × 20 mm (1024 × 1024)
Pixel size	28 μm	20 μm
Max. Frame Rate	16.6 kHz	7.5 kHz
Lens	Nikon	Nikon
Focal length	160 mm	160 mm
Diagonal FOV	60 mm	60 mm
Resolution	40 μm/Pixel	107 μm/Pixel

Results

The observation of the interaction between a single spray jet with an oil film of a thickness of 80 μm is initially carried out with a Phantom V1612 color camera. The aim is to detect the color marking of the fuel and the oil. Furthermore, the detection of splashing and secondary droplets will be observed. Subsequently, the composition of the secondary droplets is to be observed with the optical separation of the fuel and oil tracers, using two monochrome HSS6 high-speed cameras. The basic experimental setup is shown in Figure 6 and Table 2 shows the image properties of both setups.

Polychrome pictures

The visualization of the spray-oil film interaction by means of the polychrome camera is shown in Figure 9. With an exposure time of 57 μs and a frame rate of 16.6 kHz every tenth image is shown, resulting in a time step of about 600μs between images. Furthermore, the origin and directions of the X and Y coordinates are introduced in in Figure 9–1, and the impact angle is set to 45°. It can be seen that at the beginning of the interaction (Figure 9–2), a fog forms in the positive X direction. This contains a large number of very small droplets moving parallel to the surface of the oil film at a speed of about 15 m/s. Their composition is initially not clearly visible. Their movement led to the assumption, that the incoming fuel jet must indicate a flow in the initially calm atmosphere to positive X-direction, which accelerates the secondary droplets. The following pictures show that the incoming spray induces a wave into the oil film with a maximum wave height of about 600 μm. Subsequently, larger drops can be observed (Figure 9–4/5/6/7). These also move approximately parallel to the film surface, even if some drops show a slight up and down movement. In addition, some drops can be observed that settle on the oil film and are subsequently not further detectable. The velocity of the larger drops, which can have a size of approx. 40–360 μm, seems to be lower (approx. 10 m/s) compared to the fog observed at the beginning. Moreover, the formation of the large drops can be analyzed very well. From the induced wave peaks, due to the induced flow, the observable large drops are detached. In the process, fuel droplets accumulate on the surface until
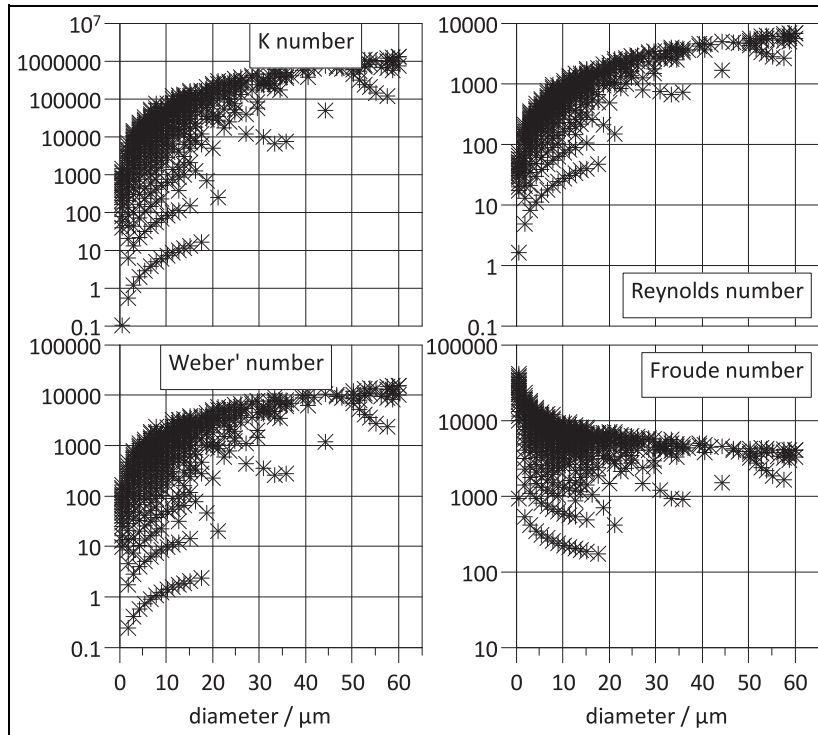
Figure 8. Distribution of the dimensionless numbers K-, Re, We′, and Fr for the used fuel spray.
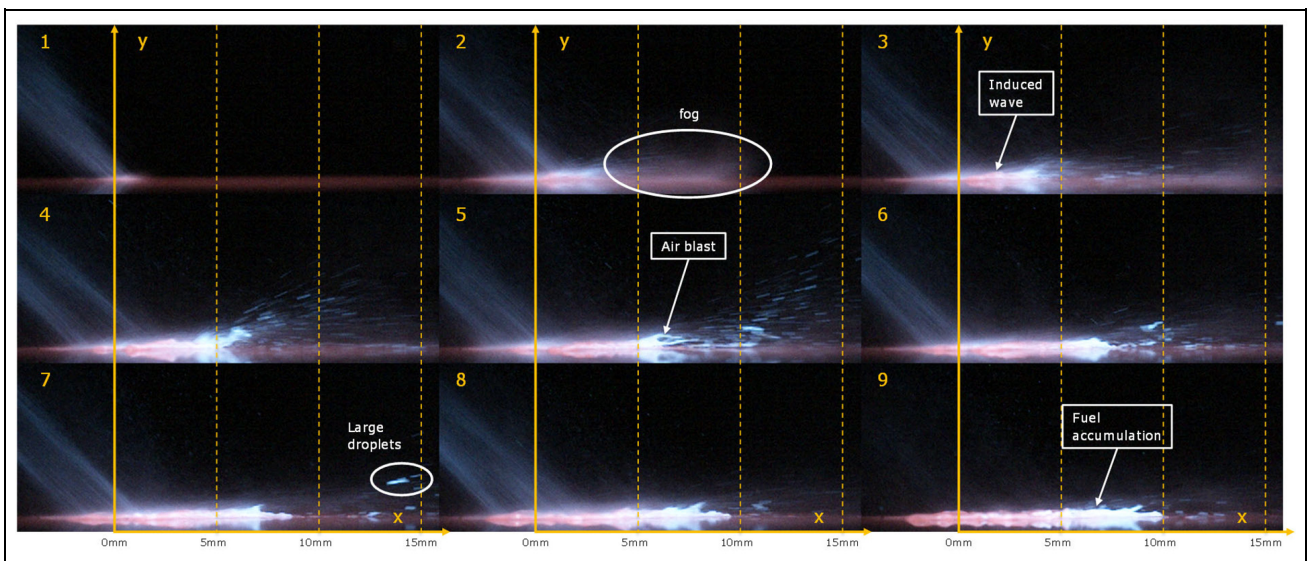

Figure 9. Polychrome, highspeed images of the interaction between a single fuel jet and an oil film with a thickness of 80μm.

they are detached by the induced flow in the X direction. The description of the formation mechanism of these droplets, could be derived from the model of Roisman et al.,[20] since partially comparable properties can be observed. The initially stationary atmosphere is accelerated by the injection in the X-direction and therefore the oil film and especially the induced waves are locally affected by a flow or shear force, which leads to the detachment of the large secondary droplets. Moreover,

the droplet size is much higher compared to the primary spray. However, compared to Roisman et al, drops larger than the oil film thickness can be observed here. Furthermore, it can be observed that the formation area of the large secondary droplets is between +5 and +7 mm in the X-direction (Figure 9–4/5). This can be seen as a further indication that this is an air-blast detachment. The color characteristics of the droplets lead to the assumption that they contain a
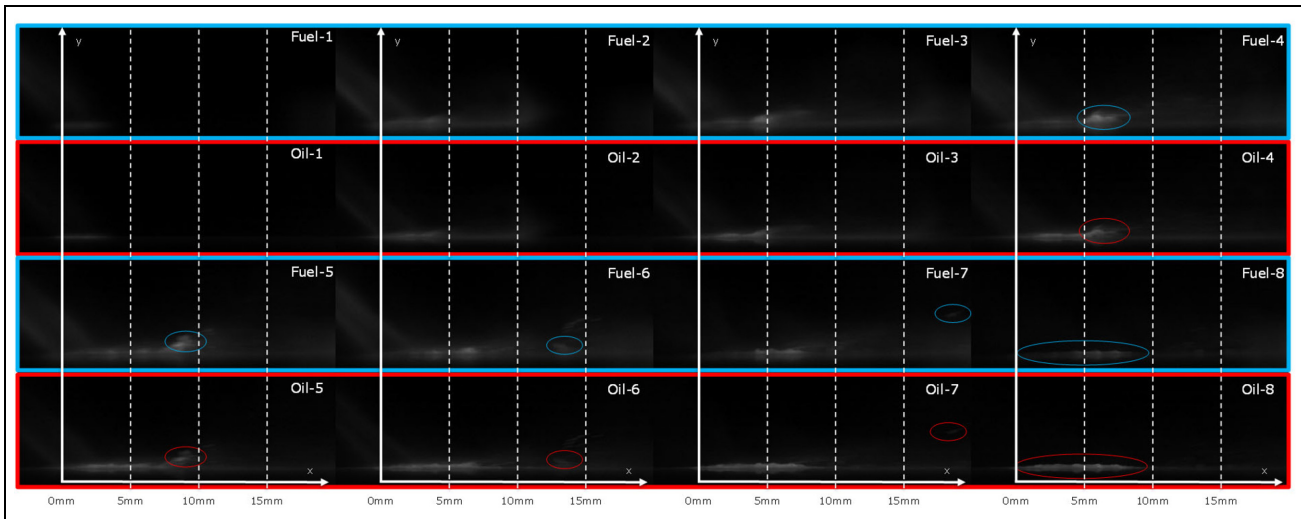
Figure 10. Monochrome, highspeed images of the interaction between a single fuel jet and an oil film with a thickness of 80μm; fuel containing components are outlined in blue, oil containing components are outline in red.

significant amount of fuel. After the impact, a local accumulation of the fluid can be observed and thus the oil film can no longer be regarded as a uniform liquid film. Furthermore, in the area of the resulting film accumulation, a significantly increased blue content is evident, which indicates oil dilution by the fuel. The height of this fluid accumulation can be estimated to approx. 400 μm.

Monochrome Cameras

The visual investigation of the spray-wall interaction with two simultaneous monochrome cameras is mainly intended to achieve conclusions about the composition during the interaction processes. The setup of cameras and optical filters is as shown in Figure 6(b). The images of the first camera visualize the fuel components (blue) while the images of the second camera highlight the oil components (red). The images are recorded with a frame rate of 7.5 kHz and an exposure time of 133.3 μs. Figure 10 shows every sixth image resulting in a time step of 800 μs between the images. The first and third rows show the images from the fuel-sensitive camera, while the second and fourth rows show the images from the oil-sensitive camera. Essentially, the four previously mentioned effects will be considered: Droplet fog at the beginning of the interaction, induction of the waves during the interaction, formation of the large secondary droplets and the resulting accumulation of the oil film after the interaction.

The droplet fog, which can be seen approx. 800μs after the start of the spray impact can clearly be seen in Figure 10–2 (fuel and oil). This may indicate that this fog contains both fuel and oil components. Whether it is many small mixture droplets or a distribution of small oil and fuel droplets cannot be determined with these investigations. However, the oil

content of this fog in particular can be seen as an indication that these droplets are the result of splashing effects.

The induced wave resulting from the spray impact (Figure 10–(3 to 8)) also contains significant blue and red components. It can be seen that during the entire impact process, the oil-containing components are more clearly visible and more consistently distributed (from 0 to +8 mm) in the X-direction. It can be seen that fuel components accumulate on the oil surface during the interaction, but their distribution varies temporally. While the fuel accumulates with high concentration in the range of +5 to +7mm at the beginning of the interaction (Figure 10-Fuel-3/4), it distributes more evenly in the further course of the interaction (Figure 10-Fuel-5/6) between 0 and +8mm.

And even the large secondary droplets, which are air-blast droplets as a result of the induced gas flow on the film surface, seem to contain both blue and red components according to Figure 10-Fuel/Oil-5/6/7. The red and blue circles show that the same droplet can be observed in both cameras, however, the blue portion is more visible than the red. However, conclusions about the mixing ratio of the secondary droplets cannot be made using the current setup. Both fluid fractions are also evident at the droplet's detachment point, the crest of the wave. This may indicate that parts of both fluids mix locally during the impact and therefore both parts can be observed in the air-blast drops.

In conclusion, the resulting liquid accumulation observed Figure 10-Fuel/Oil-7/8 is partially visible in both cameras. The oil portion can be seen more clearly. The fuel accumulation at the oil film surface is barely visible at X = 0mm, but it increases significantly in positive X direction. This can be explained by the fact that after injection is complete, while no further fuel

enrichment takes place, the gas flow moves the fuel in the X direction due to the low viscosity.

Summary and conclusions

In this work, an experimental setup was described that allows the interaction of a fuel spray and an oil-wetted wall to be investigated under reproducible and engine-relevant conditions. For this purpose, a suitable pressure chamber, an oil film generator and a single-hole injector were developed. Furthermore, the optical setup was the main focus with regard to the measurement technology. A suitable pair of fuel and oil tracers was found, both of which could be excited in a similar UV spectrum and at the same time had such a different Stokes shift that they could be separated optically. This was done on the one hand with a polychrome camera, in whose images the fuel is shown in blue and the oil in red. In addition, a dichroic filter was used to direct the blue fluorescent light to one camera and the red light to a second monochrome camera, which allows better understanding of the composition during the interaction. Four main phenomena were observed: Shortly after the beginning of the interaction a fog can be seen, which consists of many very small droplets. This seems to contain both fuel and oil components. Furthermore, the impact induces a wave in the initially stationary oil film. The maximum height of the wave can be many times the original oil film thickness. In the further course of the interaction, large secondary drops can be seen, which can be larger than the oil film thickness. Moreover, these droplets seem also to contain both fuel and oil components. The cause is assumed to be a shear force as a result of the induced gas flow in the X-direction, which behaves similarly to an air-blast detachment. Finally, it can be observed that after the interaction, a local accumulation of oil can be observed. Even a local fuel accumulation at the surface of the oil is clearly visible. For future optimization of the visual investigation of a fuel-oil film interaction presented here, the local resolution can be improved by using long-distance-microscopy. Furthermore, the surface accumulation of fuel on the oil film can be detected by an additional low-speed camera. Also, varying the impact conditions, such as impact angle, fuel pressure, fluid temperatures, etc., and their influence on the interaction processes could significantly improve the physical understanding of these phenomena.

Declaration of conflicting interests

The author(s) declared no potential conflicts of interest with respect to the research, authorship, and/or publication of this article.

ORCID iDs

Malki Maliha https://orcid.org/0000-0002-6464-0088
Heiko Kubach https://orcid.org/0000-0001-6706-8892

Supplemental material

Supplemental material for this article is available online.

References

1. Singh E, Mubarak Ali M, Ichim A, et al. Effect of mixture formation and injection strategies on stochastic pre-ignition. SAE technical paper, 2018-01-1678, 2018.
2. Palaveev S, Magar M, Kubach H, Schiessl R, Spicher U and Maas U. Premature flame initiation in a turbo-charged DISI engine - numerical and experimental investigations. *SAE Int J Engines* 2013; 6(1): 54–66.
3. Weidenlener A, Pfeil J, Kubach H, et al. The influence of operating conditions on combustion chamber deposit surface structure, deposit thickness and thermal properties. *Automot Engine Technol* 2018; 3(3-4): 111–127.
4. Kubach H, Weidenlener A, Pfeil J, et al. Investigations on the influence of fuel oil film interaction on pre-ignition events in highly boosted DI gasoline engines. SAE technical paper, 2018-01-1454, 2018.
5. Zöbinger N and Lauer T. Numerical Investigation of the influence of oil dilution on the ability to initiate a Pre-Ignition combustion. *SAE Int J Adv Curr Pract Mobil* 2020; 2: 1935–1962.
6. Richter B. *Charakterisierung der Tropfen-Wand-Interaktion im Parameterbereich von Ottomotoren mit Direkteinspritzung*. Karlsruhe: Logos-Verlag, 2007.
7. Cossali GE, Coghe A and Marengo M. The impact of a single drop on a wetted solid surface. *Exp Fluids* 1997; 22(6): 463–472.
8. Roisman IV and Tropea C. Impact of a drop onto a wetted wall: description of crown formation and propagation. *J Fluid Mech* 2002; 472: 373–397.
9. Kittel HM, Roisman IV and Tropea C. Outcome of drop impact onto a liquid film of different viscosities. In: *ILASS - Europe 2016, 27th Annual Conference on Liquid Atomization and Spray Systems*, Brighton, UK, 4–7 September 2016. pp. 4–7.
10. Kittel HM, Roisman IV and Tropea C. Splash of a drop impacting onto a solid substrate wetted by a thin film of another liquid. *Phys Rev Fluids* 2018; 3(7): 073601.
11. Sivakumar D and Tropea C. Splashing impact of a spray onto a liquid film. *Phys Fluids* 2002; 14(12): L85–L88.
12. Gianpietro C, Marengo M and Maurizio S. Impact of single and multiple drop array on a liquid film. In: *19th Annual meeting of ILASS*, Nottingham, ILASS Europe, 2004, pp.1–8.

13. Liang G and Mudawar I. Review of mass and momentum interactions during drop impact on a liquid film. *Int J Heat Mass Transf* 2016; 101: 577–599.

14. Yarin AL. Drop impact dynamics: splashing, spreading, receding, bouncing…. *Annu Rev Fluid Mech* 2006; 38: 159–192.

15. Roisman IV, Horvat K and Tropea C. Spray impact: rim transverse instability initiating fingering and splash, and description of a secondary spray. *Phys Fluids* 2006; 18: 102104.

16. Liang G, Guo Y, Shen S and Yu H. A study of a single liquid drop impact on inclined wetted surfaces. *Acta Mech* 2014; 225(12): 3353–3363.

17. Liang G, Guo Y, Yang Y, Zhen N and Shen S. Spreading and splashing during a single drop impact on an inclined wetted surface. *Acta Mech* 2013; 224(12): 2993–3004.

18. Sikalo S, Tropea C and Ganić EN. Impact of droplets onto inclined surfaces. *J Colloid Interface Sci* 2005; 286(2): 661–669.

19. Bisighini A and Cossali GE. High-speed visualization of interface phenomena: single and double drop impacts onto a deep liquid layer. *J Visual* 2011; 14(2): 103–110.

20. Roisman IV, Tropea C and Batarseh FZ. Chaotic disintegration of a liquid wall film: A model of an Air-Blast Atomization. *Atomization Sprays* 2010; 20: 837–845.

21. Opfer L, Roisman IV and Tropea C. Primary atomization in an airblast gas turbine atomizer. In: Opfer L, Roisman IV and Tropea C (eds) *Flow and combustion in advanced gas turbine combustors*. Dordrecht: Springer, 2013, pp.3–27.

22. Pranav K. *Fundamentals and techniques of biophysics and molecular biology*. New Delhi: Pathfinder Publication Unit of PAPL, 2016.

23. Rüttinger S, Spille C, Hoffmann M and Schlüter M. Laser-induced fluorescence in multiphase systems. *ChemBioEng Rev* 2018; 5(4): 253–269.

24. Schweizer T, Kubach H and Koch T. Investigations to characterize the interactions of light radiation, engine operating media and fluorescence tracers for the use of qualitative light-induced fluorescence in engine systems. *Automot Engine Technol* 2021; 6: 275–287.

25. Fuhrmann D, Benzler T, Fernando S, et al. Self-quenching in toluene LIF. *Proc Combust Inst* 2017; 36(3): 4505–4514.

26. Müller T and Poll G. Simultane Visualisierung von Öl- und Kraftstoffschichten in der Kolbengruppe eines direkteinspritzenden Ottomotors durch laserinduzierte Fluoreszenz. Dissertation, University Duisburg-Essen, 2018.

27. van der Kley S, Einspieler V, Goet G, et al. Oil film thickness and temperature measurement method for in-situ diagnostics. ECM, 2021.

28. Maliha M, Kubach H and Koch T. Comparison of spray formation a multi and a single hole gasoline direct injector. In: *Proceedings of the ASME 2021*, ICEF2021–67827, 2021.

Appendix

Notations

CCD	combustion chamber deposits
d	droplet size
d_{AMD}	arithmetic average of droplet size
Fr	froude number
g	gravity
GDI	gasoline direct injection
h	film thickness
H	relative film thickness
H_{AMD}	arithmetic average of relative film thickness
K	K Factor
LED	light emitting diode
LIF	laser induced fluorescence
Re	Reynolds number
$RON95$	research octane number 95
u	droplet velocity
UV	ultra violet
v	dynamic viscosity
We	weber number
We'	modified weber number
We_G	weber number of the gas flow
ρ	density
σ	surface tension
Φ	impact angle